

Self-Assembly of an Amphiphilic Siloxane Graft Copolymer in Water

Yining Lin and Paschalis Alexandridis*

Department of Chemical Engineering, University at Buffalo, The State University of New York, Buffalo, New York 14260-4200

Received: November 15, 2001; In Final Form: July 8, 2002

The micelle formation and micelle structure of an amphiphilic poly(dimethylsiloxane)-graft-polyether copolymer in aqueous solution were investigated with a variety of experimental techniques. We measured the CMC by three different methods—DPH solubilization, methyl orange hypsochromic shift, and pyrene fluorescence I_1/I_3 ratio. The microviscosity was evaluated from DPH anisotropy values that were obtained by fluorescence polarization measurements. The microviscosity in the siloxane copolymer micelles was found lower than that in Pluronic block copolyether micelles. The micelle size and structure were obtained from small-angle neutron scattering (SANS) using the hard sphere model. The micelle hydrodynamic radius and the micelle size distribution were monitored by dynamic light scattering (DLS). The degree of hydration was estimated from a combination of DLS and SANS results. The temperature effect on CMC was found to be small; however, a structural transition of micelles from spheres to ellipsoids was observed by SANS at elevated temperature (60 °C).

Introduction

Silicone-containing surfactants are used in numerous applications such as polyurethane foams, cosmetics, textiles, agricultural adjuvants, coatings, and inks, because of (i) the low surface tensions (20–30 mN/m) that they exhibit, (ii) their incompatibility with both aqueous and hydrocarbon solvents, (iii) their ability to form various aggregates in water, and (iv) their relatively low toxicity.^{1–6} Despite the many applications, research publications on the self-assembly behavior of silicone-containing surfactants in water are scarce. Over the past decade, a few reports on the lyotropic phase behavior in water of trisiloxane-ethoxylate surfactants or poly(dimethylsiloxane)-graft-polyether copolymers have appeared.^{7–12} At the time that we initiated our study on this subject,¹³ we were aware of only two reports on the micellization of silicone-containing surfactants.^{14,15} Our interest in poly(dimethylsiloxane)-graft-polyether copolymers has been motivated by their potential in improving properties of waterborne coatings and ink-jet inks.^{16,17} In such formulations, as the system evolves from a high water content dispersion to a coated film (with decreasing amounts of water), siloxanes play different roles at different stages and interact to varying degrees with colloidal particles and with components of the surface on which the coating is applied. An understanding of such complex interactions passes necessarily through fundamental studies on surfactant self-assembly in aqueous solutions (such as the study reported here) and on surfactant adsorption on colloidal particles.¹⁷

In this report, we first determine using spectrophotometry the CMC in aqueous solution of a poly(dimethylsiloxane)-graft-polyether copolymer, with the polyether consisting of both ethylene oxide (EO) and propylene oxide (PO). Furthermore, we assess the local environment (micropolarity and microviscosity) in the interior of the micelles. Spectroscopic techniques based either on optical absorption or on emission of light

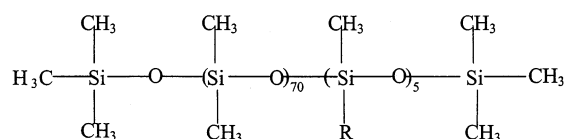


Figure 1. The structure of the poly(dimethylsiloxane)-graft-polyether copolymer considered here.

from probe molecules are well established for investigating CMC in various surfactant solutions;¹⁸ however, the suitability of hydrocarbon molecules to probe the siloxane-rich micelle interior is not yet established. We then address the structure of the micelles formed. The micelle core radius and structure evolution were investigated by small-angle neutron scattering (SANS). The micelle hydrodynamic radius and size distribution were obtained by dynamic light scattering (DLS). Finally, we consider temperature effects on the CMC, micelle size, and micelle structure.

Materials

The poly(dimethylsiloxane)-graft-polyether copolymer examined here was provided by Goldschmidt AG, Essen, Germany, and has the chemical formula (shown in Figure 1) MD₇₀D'M (M: Me₃SiO_{1/2}–, D: –Me₂SiO–, D': Me(R)SiO–, R: poly(ethylene oxide)–poly(propylene oxide) (PEO–PPO) polyether) with MW = 12000. The molecular weight per polyether group in the siloxane copolymer is 1200 and the polyether composition is 75% PEO and 25% PPO (this corresponds to approximately 19 EO segments and 6 PO segments). In this copolymer 11% free polyether was present due to an excess polyether used in the synthesis; the presence of free polyether in solution is not expected to affect the siloxane copolymer micelle formation and structure since the polyether has sufficiently low molecular weight and sufficiently high PEO content to be completely water-soluble;¹⁹ moreover, the polyether is not expected to interact with the siloxane copolymer. 1,6-Diphenyl-1,3,5-hexatriene (DPH, the structure is shown in

* Author to whom correspondence should be addressed. Fax: (716) 645-3822. E-mail: palexand@eng.buffalo.edu.

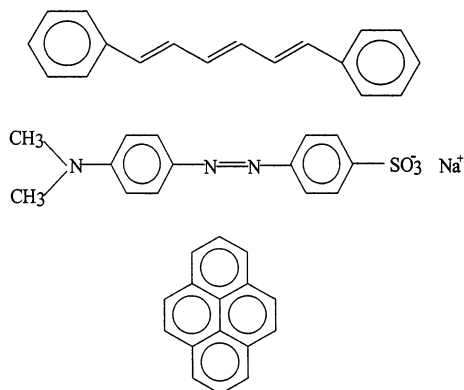


Figure 2. The structure of (top) 1,6-diphenyl-1,3,5-hexatriene; (middle) methyl orange; and (bottom) pyrene.

Figure 2a) was obtained from Molecular Probes Inc., Eugene, OR. Methyl orange 99.5% (Figure 2b) and pyrene 99% (Figure 2c) were purchased from Aldrich Co. Pluronic P105 (EO₃₇PO₅₆-EO₃₇, CMC = 0.3% at 25 °C) and Pluronic F127 (EO₁₀₀PO₆₅-EO₁₀₀, CMC = 0.7% at 25 °C) poly(ethylene oxide)-poly(propylene oxide)-poly(ethylene oxide) block copolymers were obtained from BASF Corp. All solutions (with the exception of those used for SANS) were prepared with Milli-Q filtered water (18 MΩ cm). D₂O (used in SANS) was obtained by Cambridge Isotope Laboratories Inc. (Andover, MA).

Methods

1,6-Diphenyl-1,3,5-hexatriene (DPH) UV-Vis Spectral Measurements. The rod-shaped DPH dye that is used here for the determination of the CMC is a well-known probe of lipid membrane interiors and has also been used to determine micelle formation in Pluronic PEO-PPO-PEO aqueous solutions.¹⁹ The fluorescence or absorption intensity of DPH in water is minimal, but it is substantially enhanced when associated with surfactants. A typical DPH absorption spectrum is shown in Figure 3a. The main absorption intensity peak is at 354 nm. Siloxane copolymer aqueous solutions with concentration ranging from 0.0001% to 10% w/v were prepared by diluting a stock solution to the desired concentration. The experiments were performed at 24 °C within a couple days of solution preparation. Sample preparation was as follows: a stock solution of 0.4 mM DPH in methanol was prepared; 25 μL of the DPH/methanol solution was added to 2.5 mL of copolymer solution, so that the final solution contained 0.004 mM DPH and 250 mM methanol. The amount of methanol is so low that is not expected to affect the micelle formation.^{19,20} The solutions were left in the dark to equilibrate for at least 3 h before the spectroscopic measurement. UV-vis absorption spectra of the copolymer/DPH/water samples were recorded in the 320–400 nm range using a Beckman DU-70 UV-vis spectrophotometer. The CMC value at 40 °C was measured using a Spectra Max 340 instrument.

Methyl Orange Hypsochromic Shift. Methyl orange is a solvatochromic dye molecule that has been used to investigate the formation of surfactant micelles.²¹ The noncovalent incorporation of methyl orange in the micelles is reflected by a hypsochromic shift of the long-wavelength absorption band of methyl orange.²¹ Typical methyl orange absorption spectra are shown in Figure 3b. Note the blue shift when the poly(dimethylsiloxane)-graft-polyether copolymer concentration increases from 0.01% (below CMC) to 3% (above CMC). Measurements were carried out on Beckman DU-70 UV-vis

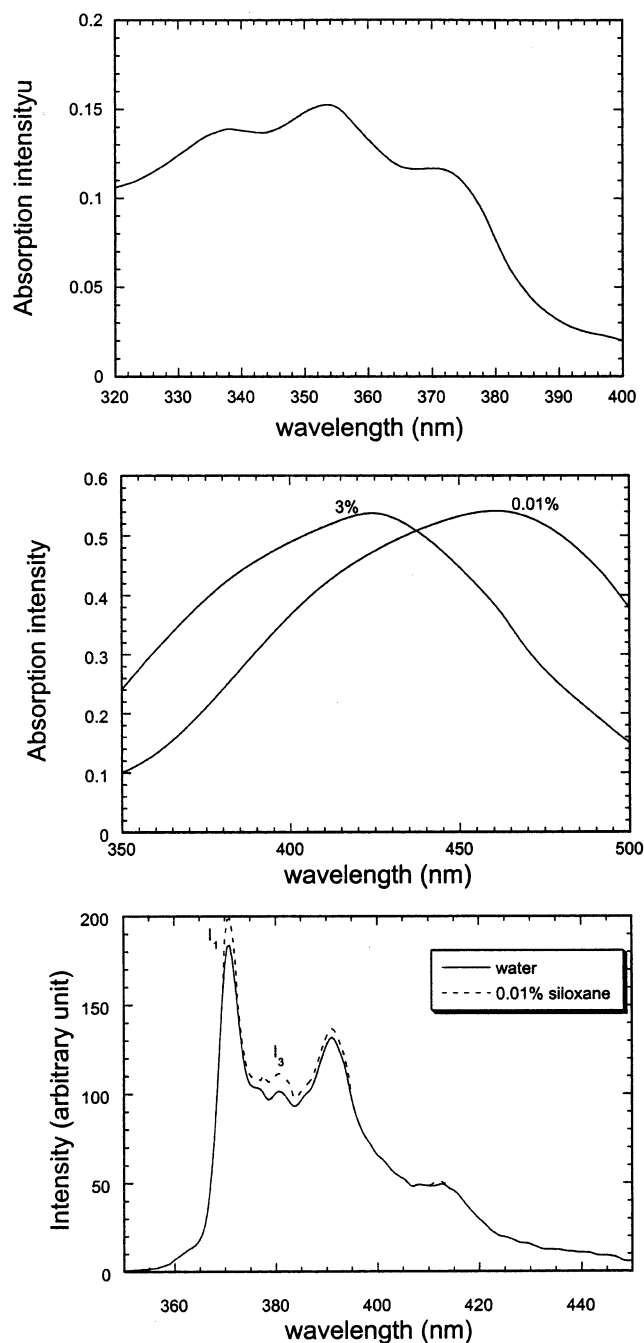


Figure 3. (top) Typical UV-vis absorption spectrum of DPH in aqueous siloxane solution (1%, above CMC). As the concentration of the siloxane copolymer (and that of micelles) increases, the intensity at λ_{354} will increase. (middle) Typical UV-vis absorption spectra of methyl orange in aqueous siloxane solution. At 0.01% siloxane (below CMC), the wavelength at which the maximum intensity is observed is 462 nm. As the siloxane copolymer concentration increases to 3%, the wavelength of the maximum will decrease, indicating the formation of micelles. (bottom) Typical fluorescence emission spectra of pyrene in distilled water and in 0.01% siloxane aqueous solution. The value of the I_1/I_3 ratio is used to indicate the polarity of the microenvironment where the pyrene is located. As the concentration of siloxane increases, the I_1/I_3 ratio will decrease as pyrene is solubilized in the micelles.

spectrophotometer. The concentration of the dye (2.5×10^{-2} mM) was kept constant.

Pyrene Fluorescence. Pyrene has been extensively used as a fluorescence probe to investigate the formation of hydrophobic microdomains by surfactants. In particular, the pyrene spectrum shows several vibronic peaks, and the ratio I_1/I_3 of the intensities

of the first and third vibronic peak is a sensitive indicator of the polarity of the pyrene microenvironment.²² Typical pyrene-fluorescence emission spectra are shown in Figure 3c. Fluorescence spectra were recorded with a Perkin-Elmer LS50 luminescence spectrometer. The excitation wavelength was 335 nm and the emission spectra were recorded from 360 to 500 nm. Pyrene was recrystallized 3 times from ethanol. A stock solution of 5 mM pyrene in acetone was prepared, from which 5 μ L were added to 4 mL of the siloxane aqueous sample. The final pyrene concentration was 6.25×10^{-3} mM and the acetone concentration was 17 mM (too low to have an effect on CMC).

DPH Anisotropy Measurements. The viscosity/mobility in the interior of surfactant assemblies can be assessed from measurements of the molecular anisotropy which results from molecular rotational diffusion. Because of the restricted rotational motion of DPH, the anisotropy increases with increasing viscosity of the microenvironment where DPH lies. The fluorescence anisotropy (r) can be related to the friction coefficient for molecule rotation according to the following equation:²³

$$\frac{1}{r} = \frac{1}{r_0} + \frac{kT\tau}{\eta V r_0} \quad (1)$$

where r_0 is the anisotropy in rigid media, k is the Boltzmann constant, τ is the lifetime of the fluorescence probe in its environment, η is the microviscosity, V is the effective volume of the probe, and T is the absolute temperature. This equation predicts a linear relationship between $1/r$ and $T\tau/\eta$. Microviscosity values often decrease as the temperature increases.

The fluorescence anisotropy of samples (4 mL) containing 40 μ L of 0.4 mM DPH was measured by a Perkin-Elmer LS50 instrument using a L-format detection geometry. The advantage of using DPH lies in its high extinction coefficient, allowing dilute solutions to be examined. The limiting anisotropy is constant from 320 to 380 nm, allowing a choice of excitation wavelengths.²³ The fluorescence anisotropy was calculated from the following relationship:

$$r = \frac{I_{VV} - GI_{VH}}{I_{VV} + 2GI_{VH}} \quad (2)$$

where $G (= I_{HV}/I_{HH})$ is an instrument correction factor, and I_{VV} , I_{VH} , I_{HV} , and I_{HH} refer to the resultant emission intensity polarized in the vertical or the horizontal detection planes (second sub index) when excited with vertically or horizontally polarized light (first sub index). The excitation wavelength was 360 nm and the emission was measured at 428 nm.

Small-Angle Neutron Scattering. SANS measurements were performed at the National Institute of Standards and Technology (NIST) Center for Neutron Research, beam guide NG3. The neutron wavelength used was $\lambda = 0.6$ nm. The sample-to-detector distance was 260.0 and 1300.0 cm. The resolution ($\Delta q/q$) was about 0.15. The angular distribution of the scattered neutrons was recorded in a two-dimensional detector; the radial average was subsequently obtained and used for data analysis. 0.01%, 0.2%, 1%, and 5% siloxane copolymer solutions were prepared in D₂O, which provides good contrast between the micelle and the solvent. The samples were placed in 1 mm path length stopped “banjo” quartz cells, and scattering data were recorded at different temperatures in the range. Adequate time was allotted for thermal and kinetic equilibration. Scattering intensities from the copolymer solution were corrected for detector background, empty cell scattering, and sample trans-

mission as described in ref 24. The resulting corrected intensities were normalized to absolute cross section units.

SANS Data Analysis. The absolute SANS intensity can be expressed as a product of $P(q)$, related to the form factor, and the structure factor $S(q)$:²⁴

$$I(q) = NP(q)S(q) \quad (3)$$

where N is the number density of the scattering particles, in our case micelles, which depends on the copolymer concentration and the association number of micelles. The particle form factor $f(q)$ is related to $P(q)$ by the following expression:

$$P(q) = [V_p(\rho_p - \rho_s)f(q)]^2 \quad (4)$$

where V_p is the micelle particle volume, and ρ_p and ρ_s are the mean scattering length density (SLD) of the micelle particles and solvent, respectively. The form factor $f(q)$, which takes into account the intramicelle structure, depends on the shape of the colloidal particle. The hard sphere form factor that describes a dense spherical particle with radius R is given by

$$f(q) = 3[\sin(qR) - qR \cos(qR)]/(qR)^3 \quad (5)$$

In fitting the hard sphere model into the scattering data, we view the micelle particles as consisting of a “dry” core (composed of siloxane and PPO segments with little or no solvent present) and a hydrated corona consisting of solvated PEO segments. When the siloxane solutions are prepared in D₂O, the contrast between the micelle core, with low SLD ($\rho_{\text{siloxane}} = 6.58 \times 10^{-8} \text{ \AA}^{-2}$ and $\rho_{\text{PPO}} = 3.25 \times 10^{-7} \text{ \AA}^{-2}$), and the solvent, with high SLD ($\rho_{\text{D}_2\text{O}} = 6.33 \times 10^{-6} \text{ \AA}^{-2}$), is good, but the contrast between the hydrated corona and the solvent (water) is poor. Therefore, $P(q)$ mainly depends on the hydrophobic core, and the radius R obtained from the hard sphere form factor fit corresponds to the micelle core radius. For a dilute solution, the structure factor is close to unity. With an increase in the copolymer concentration, a correlation peak will arise due to the intermicellar structure factor. In our data, we did not observe the peak and therefore we assume $S(q) = 1$. We thus fitted the scattering data obtained from 0.01% to 5% solutions using the hard sphere form factor, with only one fitting parameter (R).

Dynamic Light Scattering. Dynamic light scattering measures the time-dependent scattering intensity emanating from the sample which leads to the correlation function $G^{(2)}(\Gamma)$ obtained by means of a multichannel digital correlator.²⁵

$$G^{(2)}(\Gamma) = A(1 + b|g^{(1)}(\tau)|^2) \quad (6)$$

where A , b , τ , Γ , and $|g^{(1)}(\tau)|$ are the baseline measured by the counter, coherence factor, delay time, decay rate, and normalized electric field correlation function, respectively. In our study $|g^{(1)}(\tau)|$ was analyzed by the exponential sampling (EXPSAM) method, yielding information on the distribution function of Γ , $G(\Gamma)$. $G(\Gamma)$ is used to determine an average (translational) diffusion coefficient $D_{\text{app}} = \Gamma/q^2$ where $q = (4\pi n/\lambda) \sin(\theta/2)$ is the scattering wave vector. The apparent hydrodynamic radius R_h is related to D_{app} via the Stokes–Einstein equation:

$$D_{\text{app}} = kT/6\pi\eta R_h \quad (7)$$

where k is the Boltzmann constant, T is the absolute temperature, and η is the viscosity of the solvent.

We used a Brookhaven BI-200SM goniometer with a Lexel model 95 argon ion laser to obtain the micelle size distribution from a plot of $G(\Gamma)$ versus R_h by the correlation data with the EXPSAM fitting routine, with $G(\Gamma_i)$ being proportional to the scattering intensity of particle i having an apparent hydrodynamic radius $R_{h,i}$. The copolymer concentrations studied at 24 °C were 1%, 2%, and 5%, all higher than the CMC (see discussion below).

Results and Discussion

CMC Determination. UV-vis spectra of aqueous siloxane solutions containing DPH with siloxane concentrations in the range 0.0001 to 10% w/v were recorded at 24 °C. At low concentrations the siloxane did not associate in aqueous solution and DPH was not solubilized in a hydrophobic environment, therefore, the UV-vis intensities of DPH were very low. At higher concentrations, the siloxanes formed micelles and DPH were solubilized in the hydrophobic micelle interior, giving a characteristic spectrum (Figure 3a). The CMC values for siloxane copolymer in aqueous solution of various concentrations were obtained from the first inflection of the absorption intensity at 354 nm vs siloxane concentration plot for DPH probe (Figure 4a), as established in ref 19. The arrow on the plot indicates the evaluated CMC (0.05%).

The UV-vis spectra of methyl orange in 0.0001–10% (w/v) siloxane copolymer solutions were used to construct a λ_{\max} versus siloxane concentration plot (Figure 4b). The spectra (Figure 3b) of methyl orange remain unaltered in the presence of siloxane up to a certain siloxane concentration, but a progressive blue shift in λ_{\max} was observed at high concentration, also up to a certain value. In Figure 4b, the absence of any change in λ_{\max} in the dilute region indicates that the copolymer remains fully dissolved in water and does not affect the spectrum of the dye. At higher concentrations, the siloxane forms hydrophobic domains and the dye can be considered to partition from water to these domains resulting in decrease in λ_{\max} . The CMC value for siloxane copolymer of various concentrations was obtained from the first inflection of the concentration plot (Figure 4b) with hypsochromic shift of the long-wavelength absorption bands of methyl orange. The arrow on the plot of Figure 4b points out the evaluated CMC value that is equal to 0.05%, the same as that obtained by DPH as discussed above.

A characteristic property of pyrene, which indicates the polarity of the environment in which it is solubilized, is the ratio of the intensity of its fluorescence peaks at 373 nm (I_1) and 383 nm (I_3). The change in the I_1/I_3 ratio of pyrene in the copolymer solution over the 0.0001 to 20% (w/v) concentration range is shown in Figure 4c. As pyrene binds to hydrophobic sites, the I_1/I_3 ratio is reduced by a factor characteristic of the particular microenvironment where the pyrene molecules are located. Taking into account (i) the CMC value from the DPH and methyl orange experiments reported here, and (ii) our previous studies on the micellization of Pluronic PEO–PPO–PEO block copolymers where several techniques were calibrated to determine the CMC,²⁶ the second inflection of the concentration plot for pyrene I_1/I_3 was assigned to the CMC as detected by pyrene. Note that the I_1/I_3 ratio started decreasing already at a siloxane concentration of 0.002%. A similar behavior has been observed in Pluronic block copolymer aqueous solutions,²⁶ and may be due to pyrene molecules sensing/reporting the hydrophobic environment generated by single (nonassociated) copolymer molecule that are in a coiled conformation. As alluded to in the Introduction, the use of dye molecules as such reported

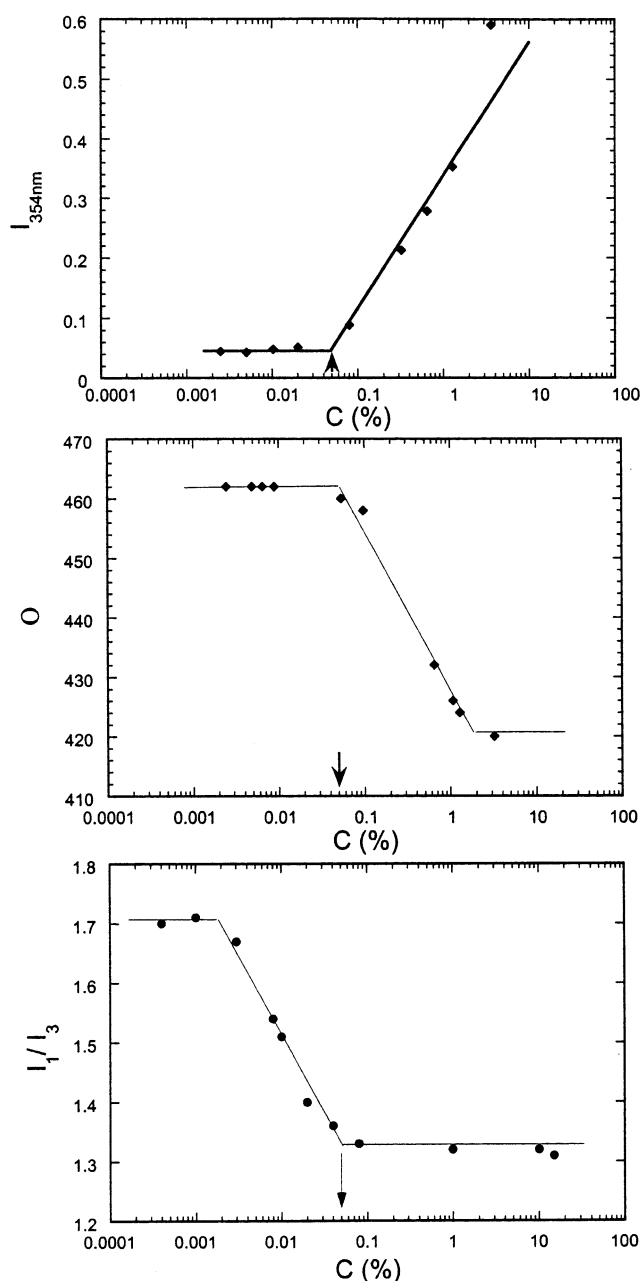


Figure 4. (top) UV-vis intensity at 354 nm (due to DPH) of aqueous siloxane solutions with concentrations in the range 0.0001 to 10%. At low concentrations, the siloxane did not associate in aqueous solution and DPH was not solubilized in a hydrophobic environment. Therefore, the UV-vis intensities due to DPH were very low. At higher concentrations, the siloxanes formed micelles and DPH was solubilized in the hydrophobic micelle interior. We choose the inflection point as the CMC (0.05%). (middle) The UV-vis spectra of methyl orange at a concentration 2.5×10^{-5} M for siloxane copolymer solution over the 0.0001–10% were used to construct λ_{\max} versus surfactant concentration plots. The spectrum of the dye remains unaltered in the presence of siloxane up to a certain concentration, but a progressive blue shift in λ_{\max} is observed at high concentration also up to a certain value. The CMC value for siloxane copolymer at various concentrations was obtained from the first inflection of the plot of the hypsochromic shift of the long-wavelength absorption bands of methyl orange vs the siloxane concentration. The arrow on the plot points out the CMC value (0.05%). (bottom) Changes in the I_1/I_3 ratio of pyrene plotted vs the siloxane concentrations in the range 0.0001 to 10% (w/v). As pyrene binds to hydrophobic binding sites in surfactant aggregates, the I_1/I_3 ratio is reduced by a factor characteristic of the particular microenvironment where the pyrene molecules are located. The CMC value was obtained from the second inflection of the concentration plot for pyrene I_1/I_3 ratio (indicated by the arrow).

here, while well established in hydrocarbon surfactants, is new for the case of silicone surfactants, and it is potentially problematic given that hydrocarbon and silicone are immiscible. The observations reported here point to the need for further studies on the suitability of various hydrocarbon probe molecules for the characterization of silicone-containing surfactants and polymers.

CMC values for trisiloxane-ethoxylate surfactants have been reported around 0.08–3% (at 25 °C) and the CMC values were usually smaller when the EO block was smaller.²⁷ CMC values of graft copolymers with long siloxane backbones reported in ref 14 are in the range 5×10^{-4} to 0.5%. One rake-type siloxane with a structure similar to ours but with lower molecular weight (MD₁₈D'₅M, R = (CH₂)₃EO₁₂OH) has CMC equal to 5×10^{-4} %, much smaller than the CMC value determined here. These CMC values, however, were estimated by surface tension measurements, which can be very sensitive to hydrophobic impurities often present in siloxanes. In fact, a very recent study²⁸ on the micellization of MD₁₃D'₅M with R = (CH₂)₃-EO₁₂OH and of MD₂₀D'₅M with R = (CH₂)₃EO₁₀PO₄OH reports CMCs in the range 0.02–0.05%, very similar to the CMC value reported here for MD₇₀D'₅M with R = (CH₂)₃EO₁₉-PO₆OH, with much higher siloxane molecular weight but also a higher number of EO segments.

Local Polarity. The changes in the I_1/I_3 ratio of pyrene in the aqueous siloxane solutions also indicate the micropolarity of the copolymer assembly. The plateau value of I_1/I_3 in the siloxane solution at concentrations above the CMC is higher than in conventional ionic surfactant micelles, indicating that the pyrene is possibly solubilized near the hydrophobic/hydrophilic boundary in the micelles (and/or some pyrene remains outside the micelles). The concentration range between the two I_1/I_3 ratio plateaus is 0.05%–0.3% for sodium dodecyl sulfate (SDS) aqueous solutions,²⁸ but 0.002%–0.5% for the siloxane copolymer examined here. The broader transition region at the siloxane I_1/I_3 curve compared to that of SDS indicates the lower capacity of siloxane copolymer aggregates to solubilize pyrene³⁰ (recall that the CMC reported by DPH solubilization coincided with the second, higher concentration, transition reported by the pyrene I_1/I_3 ratio). In studies where pyrene was solubilized in micelles formed by Pluronic PEO–PPO–PEO block copolymer (Pluronics P104 and F108, with PPO segments in the hydrophobic micelle core), the pyrene I_1/I_3 ratio was found about 1.4 at 45 °C.^{22,26} The I_1/I_3 ratio in the siloxane micelle core is about 1.3 at room temperature, suggesting that the siloxane micelle core is more hydrophobic than the PPO core, especially at room temperature (PPO becomes more hydrophobic when temperature increases). Note, however, that the difference of I_1/I_3 ratio values between the two plateaus is about 0.6 for Pluronics P104 and F108 and that of siloxane copolymer is about 0.4. Again, this indicates the lower capacity of siloxane micelles (compared to the Pluronic P104 and F108 micelles) to solubilize pyrene.

Microviscosity. At a given temperature, the anisotropy shift, according to the Perrin equation (eq 1), can originate from either a change in the rotational correlation time, due to a viscosity change of the local environment, or a change in the fluorescence lifetime. The anisotropy data alone do not allow a quantitative separation of two effects. However, a change in the anisotropy will be observed only if the local environment in the vicinity of the probe molecule inside the micelle is altered. Therefore, the observed anisotropy change is a clear indication of solvent partitioning into the micelle phase and very possibly lowering the microviscosity of the local environment.

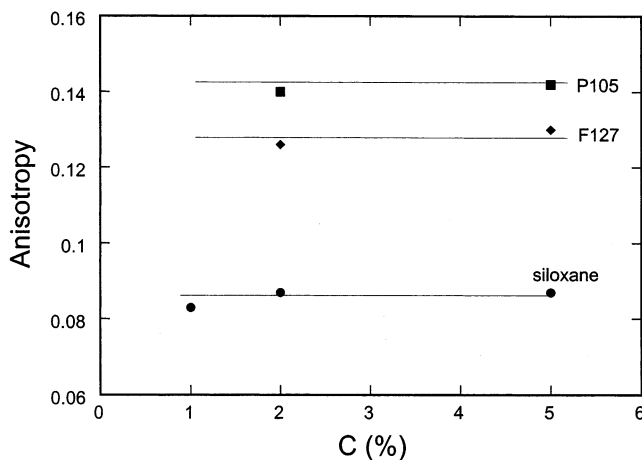


Figure 5. DPH anisotropy values for micelles formed by different copolymer types and concentrations (see text for copolymer notation). The DPH anisotropy values are independent of the copolymer concentration (above CMC) within the experimental error.

DPH anisotropy values for poly(dimethylsiloxane)-graft-polyether copolymer aqueous solutions (above the CMC), as well as for Pluronic P105 and Pluronic F127 aqueous solutions (obtained for comparison purposes) are shown in Figure 5. The DPH anisotropy values are independent of the copolymer concentration (above CMC) within the experimental error. The anisotropy value is 0.085 for the siloxane copolymer. The anisotropy values are 0.14 for Pluronic P105 and 0.13 for Pluronic F127. The lower value of the anisotropy for the siloxane micelles indicated that the siloxane copolymers do not pack as tightly as Pluronic copolymers and the DPH molecules are more mobile in siloxane micelles. The more loosely packed siloxane micelles compared to Pluronic micelles are also reflected in the differences in I_1/I_3 ratio between the two plateaus as discussed previously in the local polarity section.

Micelle Structure and Association Number. Figure 6, parts a and b, show the SANS data obtained from aqueous (D₂O) siloxane copolymer solutions and the model fits. We fitted the data for 0.01%, 0.2%, 1%, and 5% siloxane solutions using the hard sphere form factor. As shown in Figure 6, the model curve fits well the scattering data in the q range 0.01 Å⁻¹ to 0.1 Å⁻¹ (the fit could have been better if we had used a more complicated model for the form factor; however, we felt that the simple hard sphere form factor is adequate for the system considered here). The micelle core radius obtained from the fit is 75(±1) Å at all siloxane copolymer concentrations considered (see also Table 1). The ±1 Å error reported above for the micelle core radius is based on the variation of R that would result in a noticeable worsening of the fit (and not by repeat experiments at the same concentration). The increase in the scattering intensity observed with increasing siloxane concentration is due to the increase in the number density of micelles. At 0.01% siloxane solution, which is below the CMC detected by the spectroscopic methods discussed earlier, we expected to obtain the unimer structure information. However, it was not possible to fit the scattering data with the form factor for Gaussian coils. Instead, the data were fitted by the hard sphere form factor (Figure 6a). The radius we calculated from the fit was the same as the micelle size (obtained at higher concentrations), a fact indicative of the presence of micelles. Obviously there is an inconsistency between the information provided by the SANS pattern at 0.01% siloxane and the CMC value obtained from the DPH and methyl orange spectrophotometric measurements;

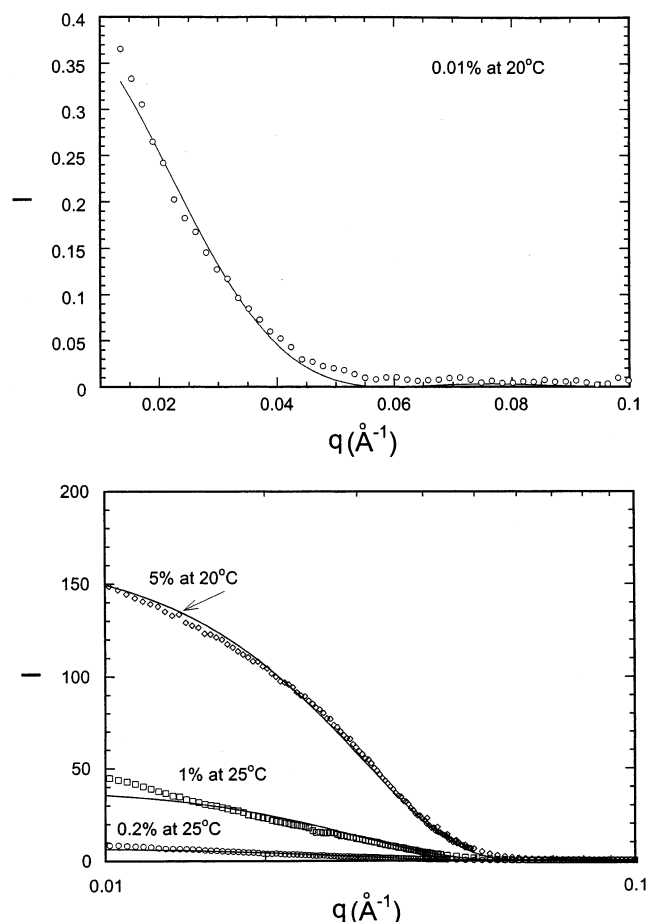


Figure 6. SANS patterns of siloxane copolymers in aqueous solution at different concentration. As the concentration increases, the scattering intensity increases. The fitted curves for (top) 0.01%, and (bottom) 0.2%, 1%, and 5% siloxane were obtained from the hard sphere form factor.

TABLE 1: The Micelle Core Radius (R) Estimated by SANS and the Hydrodynamic Radius (R_h) and Standard Deviation (σ) of the R_h Estimated by DLS at Different Siloxane Concentrations and Temperatures

concentration	temperature (°C)	R (Å)	R_h (Å)	σ (Å)
0.01%	20	75		
0.2%	25	75		
1%	25	75	121 ^a	28 ^a
2%	20		132 ^a	30 ^a
5%	20	76	131 ^a	22 ^a
5%	50		152	58
5%	60	$R_a = 160$, $R_b = 61$	229	75

^a 24 °C.

we plan to carry out further SANS experiments in order to elucidate this.

From the micelle core radius value obtained from the SANS data analysis, and under the assumptions that the micelle core consists (i) of all the siloxane and PPO segments of the copolymer molecules which participate in one micelle, and (ii) of only the siloxane and PPO blocks (i.e., there is no solvent or PEO present in the core), we can estimate the association number (average number of copolymers per micelle), $N_{\text{association}}$, as follows:

$$N_{\text{association}} = 4\pi R^3 / 3v \quad (8)$$

where v is the volume of the dimethylsiloxane plus propylene

oxide segments in one copolymer molecule ($v = 12450 \text{ Å}^3$). The $N_{\text{association}}$ thus calculated is about 142 plus/minus 6 (this error is estimated from the plus/minus 1 Å error in R). The assumption invoked in this estimation is that of strong segregation between the PEO segments and the siloxane plus PPO segments, and between the siloxane segments and the solvent.

Micelle Hydrodynamic Radius and Size Distribution. Figure 7a–c shows the size distributions exhibited by 1%, 2%, and 5% siloxane copolymer solutions in water. The size distribution data are obtained by the exponential sampling algorithm and show two well-distinguished peaks that are fitted by Gaussian curves in all conditions.²⁰ The lower size distribution, centered around 125–150 Å, corresponds to the radius of the siloxane copolymer micelles. The copolymer concentration does not show strong effect on the micelle radius, suggesting a closed-association process.³¹

The higher size distribution, centered around 500 Å (radius) with a standard deviation of about 100 Å, results from aggregates with size larger than that of micelles (possibly formed by copolymers more hydrophobic and/or of higher molecular weight than the main component). While these large aggregates contribute about 25 to 30% of the total scattered intensity, their concentration is extremely low (as we show next) and thus we did not study them further. If we convert the intensity weighted distribution to number weighted distribution via the equation:³²

$$n_i = I_i R_i^6 P(KR_i) \quad (9)$$

where n_i is relative number distribution, I_i relative intensity-weighted distribution, R_i radius corresponding to each I_i , and $P(KR_i)$ particle structure factor (assumed to be 1), then the number of particles corresponding to the higher radius peak is <0.01% of the total particles. The weight fraction of the large particles will be higher than the number fraction, but still less than 1%

Micelle Degree of Solvation. As discussed in the SANS data analysis section, water is present in the hydrated micelle corona, but the hard sphere model that we used to fit the SANS data does not account for this. However, the hydrodynamic radius of the micelles measured by DLS depends on the movement (diffusion) of the micelles, therefore the size (hydrodynamic radius) we measure in DLS should be that of the micelle core plus the solvated corona. If we consider the hydrodynamic radius, R_h , to reflect the extension into the solution of the PEO blocks of the copolymers that participate in a given micelle, we can then calculate the volume of the micelle corona as that between two concentric spheres, one defined by R_h (obtained from DLS) and the other by the micelle core radius, R (obtained by SANS). From the volume of the micelle corona we can then estimate the average number of water molecules per PEO segment, $N_{\text{solvation,PEO}}$:

$$N_{\text{solvation,PEO}} = [4\pi(R_h^3 - R^3)/3 - mN_{\text{association}}v_{\text{EO}}]/(v_{\text{water}}N_{\text{association}}m) \quad (10)$$

where m is the number of total EO monomers ($m = 100$) in one siloxane molecule, v_{EO} is the molecular volume of one PEO segment ($v_{\text{EO}} = 73 \text{ Å}^3$), and v_{water} is the molecular volume of water ($v_{\text{water}} = 30 \text{ Å}^3$). In addition to the $N_{\text{solvation,PEO}}$, we can estimate the volume fraction of PEO in the corona, $\phi_{\text{PEO,corona}}$:

$$\phi_{\text{PEO,corona}} = (mv_{\text{EO}}N_{\text{association}})/[4\pi(R_h^3 - R^3)/3] \quad (11)$$

$N_{\text{solvation,PEO}}$ and $v_{\text{PEO,corona}}$ were calculated using the $N_{\text{association}}$ value obtained above (142 ± 6) and the R_h and R values

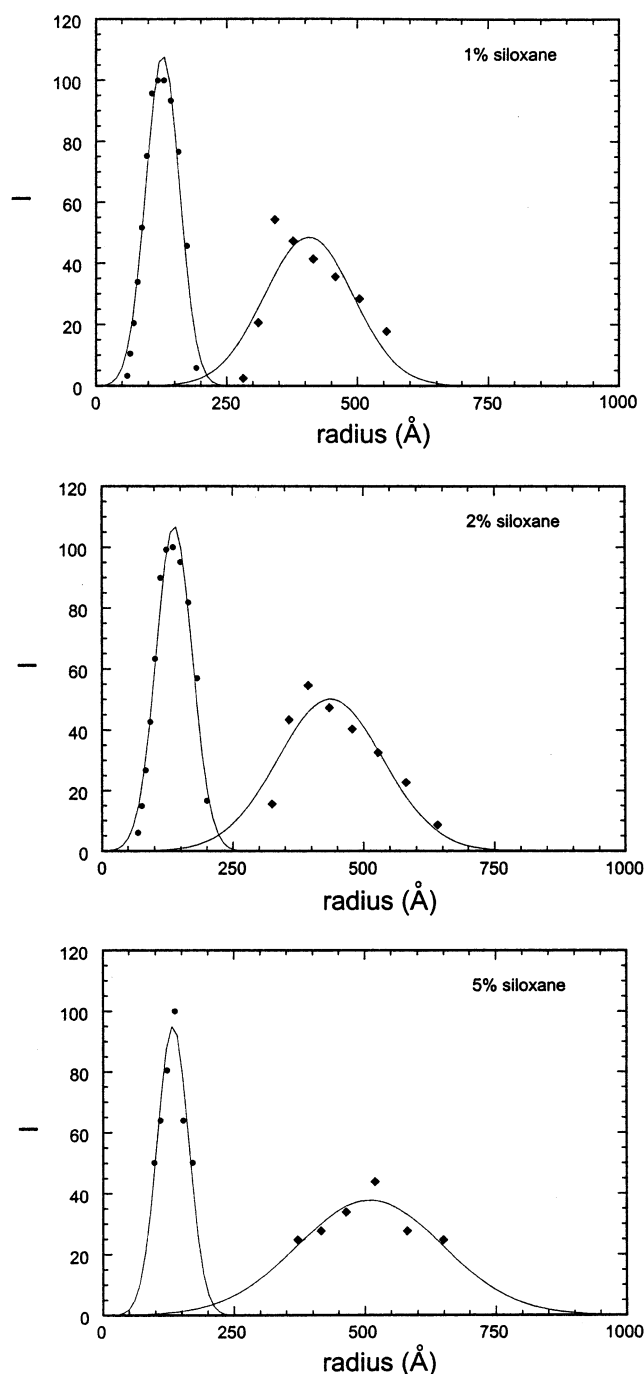


Figure 7. The intensity-fraction distribution of micelle hydrodynamic radius from (top) 1%, (middle) 2%, and (bottom) 5% siloxane copolymers in water. The data points are fitted by Gaussian curves.

obtained from the light scattering and SANS fits, respectively (125 and 75 Å). $N_{\text{solvation,PEO}}$ equals 12.6 ± 0.6 and $\phi_{\text{PEO,corona}}$ is 0.16 ± 0.01 (the errors are estimated from the error in $N_{\text{association}}$). These values are in agreement with values obtained for the PEO corona of PEO-PPO-PEO block copolymer micelles.^{22,26,33}

The intermicellar interactions are weak (as judged by the fact that $S(q) = 1$), suggesting that the micelle corona thickness is low. We now compare the chain length of fully extended polyether with the differences between R_h and R (equal to the micelle corona thickness) in order to assess if the corona is indeed formed by polyether chains. The chain length of the

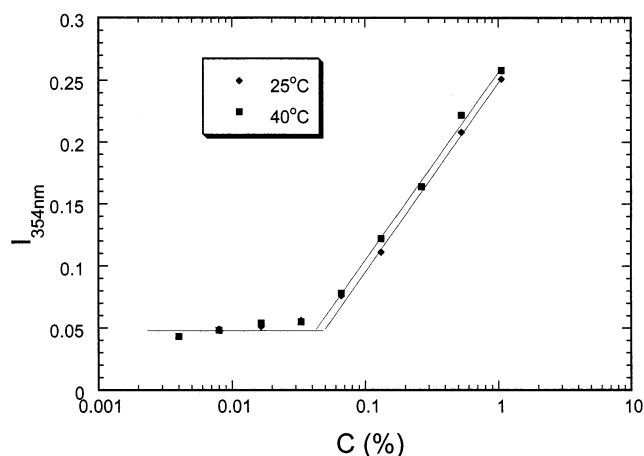


Figure 8. The dependence of CMC (detected from DPH solubilization) on temperature.

polyether group can be estimated by the following equation:³⁴

$$\langle r^2 \rangle^{1/2} = \alpha (nC_N)^{1/2} l \quad (12)$$

where $\langle r^2 \rangle^{1/2}$ is the root-mean-square end-to-end distance of a polymer coil in a random coil conformation, n is the number of bonds along the polymer backbone, α is the chain expansion factor, C_N is a parameter characteristic of the polymer ability to swell, and l is bond length (1.54 Å for C–C bond and 1.43 Å for C–O bond). If we assume C_N to be 4 and α to be 1.5,³⁴ then the calculated polyether chain $\langle r^2 \rangle^{1/2}$ is ~ 56 Å, which is close to the $(R_h - R) = 50$ Å. Therefore, the corona thickness estimated by SANS and DLS can be indeed reached by the polyether chains, even if they are in a random coil conformation (they are more likely stretched).

Temperature Effects on Micelle Formation and Structure.

The dependence of CMC on temperature was examined by the DPH solubilization technique (data are shown in Figure 8). As the temperature increases from 24 to 40 °C the CMC value of the siloxane surfactant decreases slightly from 0.05% to 0.04%. In ref 28, where a siloxane copolymer of similar structure but lower molecular weight than ours is studied, the CMC is reported to decrease from 0.034% at 25 °C to 0.016 at 45 °C. Similarly to the case of the poly(dimethylsiloxane)-graft-polyether copolymers, the decrease of the hydrophilicity of the PEO blocks with increasing temperature has comparatively little effect on the CMC as in the case of *n*-alkyl poly(ethylene glycol) ethers (CiEOj).³⁴ However, a pronounced dependence of the CMC on temperature has been observed in Pluronic PEO-PPO-PEO block copolymer solutions.^{19,35}

Figure 9 shows the size distribution (obtained by DLS) exhibited by a 5% siloxane aqueous solution at 50 and 60 °C. As temperature increases from 24 °C to 60 °C, the micelle hydrodynamic radius increases from 132 to 229 Å and the standard deviation (SD) of the micelle radius increases from 23 to 75 Å (shown in Figure 9b). The hydrodynamic radius of the large aggregates increases from 501 to 1268 Å and the standard deviation increases from 88 to 326 Å. Because the solubility of the PPO and PEO segments depends strongly on temperature, the hydrophobicity of the surfactants is expected to increase at higher temperature,³⁵ causing a decrease in interfacial tension between the micelle and water. The micelle radius therefore increases.

We also studied the temperature effects on micelle structure by SANS. As seen in Figure 10a, the scattering intensity at 40 °C coincides with the data obtained at 20 °C. As discussed

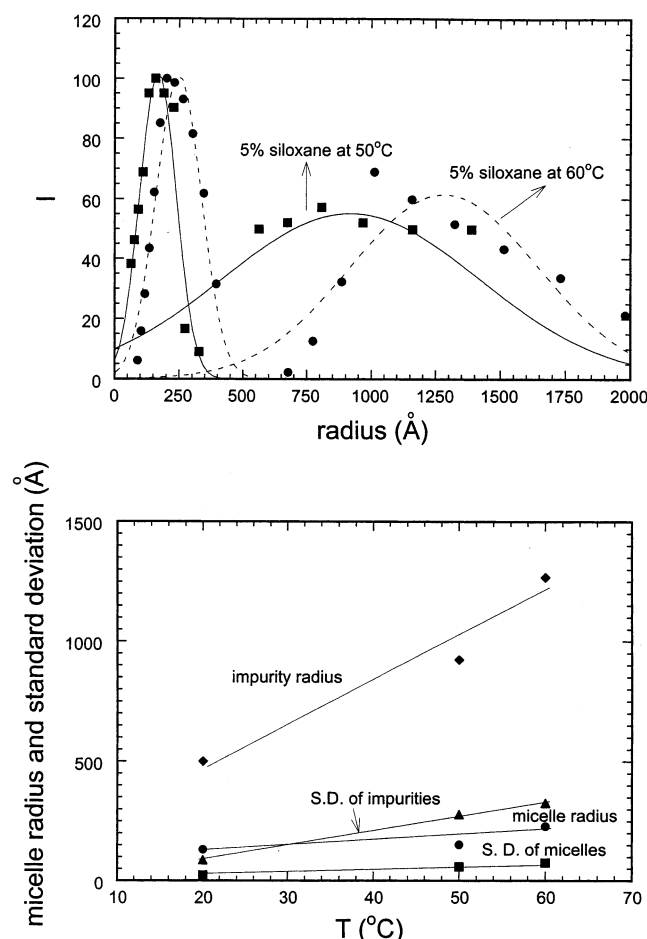


Figure 9. (top) Size distributions of 5% siloxane copolymer aqueous solutions at 50 °C and 60 °C. (bottom) As the temperature increases from 24 °C to 60 °C, the micelle radius increases from 131 to 229 Å and the standard deviation of the micelle radius increases from 22 to 75 Å.

above, the data were fitted by a hard sphere model and the obtained micelle core radius is about 75 Å. However, as the temperature increases to 60 °C, the scattering intensity increases at low q and the hard sphere form factor no longer fits well the data points (see the dashed curve in Figure 10b). Because of the low hydration and higher hydrophobicity of the PEO blocks at higher temperature, and also because of the inherent tendency of the comblike macromolecules to favor assemblies of low curvature, the micelles may grow. Under the restrictions that (i) all the headgroups are exposed to water and (ii) there is no space that is not filled with the hydrophobic chains in the micellar core, micelles will grow along one dimension (to form rods), and further to two dimensions (to form disks). We thus fitted the data at 60 °C by the monodisperse ellipsoid form factor (eq 13) with the semimajor axis R_a and semiminor axis R_b (the ellipsoid shape was selected as intermediate between sphere and cylinder). As shown in Figure 10b, the curve fits very well the data points at low q . The calculated R_a is 160 Å and R_b is 61 Å.

$$f(q) = \int_0^1 \left[\frac{(\sin(z) - z \cos(z))}{z^3} \right]^2 dx; \quad z = qR_b \left[1 + x^2 \left(\left(\frac{R_a}{R_b} \right)^2 - 1 \right)^{1/2} \right] \quad (13)$$

Note that the semiminor axis R_b is smaller than R obtained by hard spheres (76 Å), which suggests that at 20 °C the siloxane

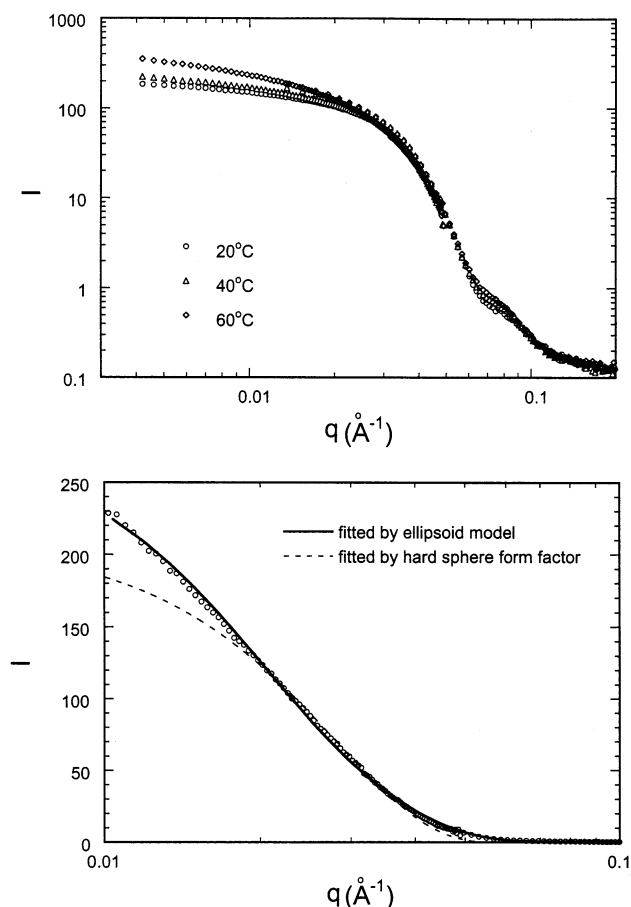


Figure 10. (top) Temperature dependence of the siloxane block copolymer structure at 20 °C, 40 °C, and 60 °C. The scattering intensities at 20 °C and 40 °C coincide. As the temperature increases to 60 °C, the scattering intensity at low q increases, indicating a transition of the micelle structure from sphere to ellipsoid. (bottom) The scattering intensity data at 60 °C were fitted by two models—the hard sphere form factor (dashed curve) and the ellipsoid form factor (solid curve). The ellipsoid form factor fits the data noticeably better at low q .

molecules could form both spherical and ellipsoid micelles. Copolymers with structure $MD_nD'R'M$ (with $R = CH_2EO_{12}OH$), $n = 13$ or 18, $m = 5$) have been found to fit the spherical models,¹⁴ but the authors suggested that the micelles of these siloxane copolymers have ellipsoidal shape with an axial ratio close to 1 and that the experimental accuracy was not sufficient to distinguish between such aggregates and exact spheres. SANS data on $MD_{13}D'M$ with $R = (CH_2)_3EO_{12}OH$ and on $MD_{20}D'M$ with $R = (CH_2)_3EO_{10}PO_4OH$, reported recently in ref 28, were fitted well to a monodisperse oblate ellipsoid model, in good agreement with the observed transition of the micelle structure from spherical to ellipsoid at higher temperature discussed above. In fact, the structural dimensions obtained in ref 28 are about 2 times lower than the ones reported here, which is reasonable given that the copolymer examined here has molecular weight twice that of ref 28.

Conclusions

CMC detection in aqueous solution of poly(dimethylsiloxane)-graft-polyether copolymer with structure $MD_{70}D'M$ (M: $Me_3SiO_{1/2}-$, D: $-Me_2SiO-$, D': $Me(R)SiO-$, R: polyether copolymer with approximately 19 ethylene oxide and 6 propylene oxide segments) in aqueous solution has been accomplished by three methods: DPH UV-vis spectra, hypso-

chromic shift of methyl orange, and pyrene I_1/I_3 ratios. The CMC value thus obtained equals 0.05% (although SANS data obtained at 0.01% siloxane copolymer provide some conflicting evidence). The microenvironment of siloxane copolymer micelles was studied by pyrene fluorescence measurements I_1/I_3 and DPH fluorescence anisotropy measurements. The microviscosity in siloxane micelles is lower than that in Pluronic PEO-PPO-PEO block copolymer micelles.

SANS experiments show that spherical micelles with association number value of about 142 are present in 5% siloxane copolymer solution at 20 °C. The micelle core has a radius of 75 Å. Dynamic light scattering data show two size distributions for the siloxane copolymer solutions, but the higher size distribution is due to only 0.01% of the particles present in solution. The peak centered at 125 Å corresponds to the micelle hydrodynamic radius. The hydrodynamic radius takes into account the core plus the corona radius, while the radius obtained from the hard sphere form factor used in fitting SANS data equals the micelle core radius; thus we can estimate the degree of solvation by relating these two radii and the micelle association number. The number of water molecules per EO segment equals 12.6 and the volume fraction of the EO segments in the micelle corona equals 0.16. The increase in temperature from 24 °C to 40 °C does not have a strong effect on the CMC of the siloxane surfactants. However, the micelle radius increases with further increase in temperature, and the SANS data indicate a structural evolution of the siloxane copolymer micelles, from spheres at 20 and 40 °C to ellipsoids at 60 °C.

Acknowledgment. We thank Xerox Foundation for partially funding this work and Dr. Thomas W. Smith (Xerox Corp.) for helpful discussions. We acknowledge the National Science Foundation (CTS-9875848) for partial support of this research. The neutron scattering facilities used in this work were provided by the National Institute of Standards and Technology (NIST) and supported by the National Science Foundation. We thank Dr. Jamie Schulz at NIST for valuable assistance with the SANS data acquisition. We thank Dr. Joachim Venzmer (Goldschmidt AG) for providing structure information on the siloxane copolymer.

References and Notes

- Schaefer, D. Silicone Surfactants. *Tenside, Surfactants, Detergents* **1990**, 27, 154–158.
- Kobayashi, R.; Reijiro, Y.; Nomura, S. Polysiloxane Gel with Low Cross-linking Density for Makeup Cosmetics. *Polym. Adv. Technol.* **1997**, 8, 351–354.
- Krupers, M. J.; Bartelink, C. F.; Gruenhauer, H. J. M.; Moeller, M. Formation of Rigid Polyurethane Forms with Semi-Fluorinated Diblock Copolymeric Surfactants. *Polymer* **1998**, 39, 2049–2053.
- Schmidt, G. Silicone Surfactants Part III. Organomodified Poly(dimethylsiloxane) as Surface Active Ingredients in Textile and Fibre Industrials. *Tenside, Surfactants, Detergents* **1990**, 27, 324–328.
- Lee, B. I.; Vergano, P. J.; Lindsay, L. Z. H.; Park, J. Silicate Modification of Corn Protein Films. *J. Mater. Sci. Lett.* **1998**, 17, 359–361.
- Hill, R. M. *Silicone Surfactants*; Marcel Dekker: New York, 1999.
- Hill, R. M.; He, M.; Lin, Z.; Davis, H. T.; Scriven, L. E. Lyotropic Liquid Crystal Phase Behavior of Polymeric Siloxane Surfactants. *Langmuir* **1993**, 9, 2789–2798.
- Stuermer, A.; Thunig, C.; Hoffmann, H.; Gruening, B. Phase Behavior of Silicone Surfactants with a Comblike Structure in Aqueous Solution. *Tenside, Surfactants, Detergents* **1994**, 31, 90–98.
- Li, X.; Washenberger, R. M.; Scriven, L. E.; Davis, H. T.; Hill, R. M. Phase Behavior and Microstructure of Water/Trisiloxane E₁₂ Polyoxyethylene Surfactant/Silicone Oil Systems. *Langmuir* **1999**, 15, 2267–2277.
- Ahn, S.; Alexandridis, P. Phase Behavior and Structural Characterization of Trisiloxane Surfactant-Water-Silicon Oil Systems. *Polym. Prepr. (Am. Chem. Soc., Div. Polym. Chem.)* **2001**, 42 (1), 169–170.
- Kunieda, H. K.; Uddin, M. H.; Horii, M.; Furukawa, H.; Harashima, A. Effect of Hydrophilic- and Hydrophobic-Chain Lengths on the Phase Behavior of A-B-Type Silicone Surfactants in Water. *J. Phys. Chem. B* **2001**, 105, 5419–5426.
- Rodriguez, C.; Uddin, M. H.; Watanabe, K.; Furukawa, H.; Harashima, A.; Kunieda, H. Self-Organization, Phase Behavior, and Microstructure of Poly(oxyethylene) Poly(dimethylsiloxane) Surfactants in Nonpolar Oil. *J. Phys. Chem. B* **2002**, 106, 22–29.
- Lin, Y.; Alexandridis, P. Microenvironment and Structure of Micelles Formed by a Polymeric Siloxane Surfactant in Aqueous Solutions. *Polym. Prepr. (Am. Chem. Soc., Div. Polym. Chem.)* **2001**, 42 (1), 229–230.
- Gradziński, M.; Hoffmann, H.; Robisch, P.; Ulbricht, W.; Gruening, B. Aggregation Behavior of Silicone Surfactants in Aqueous Solutions. *Tenside, Surfactants, Detergents* **1990**, 27, 366–379.
- Lin, Z.; Hill, R. M.; Davis, H. T.; Scriven, L. E.; Talmon, Y. Cryo Transmission Electron Microscopy Study of Vesicles and Micelles in Siloxane Surfactant Aqueous Solutions. *Langmuir* **1994**, 10, 1008–1011.
- Lin, Y.; Smith, T. W.; Alexandridis, P. Adsorption of an Amphiphilic Siloxane Graft Copolymer on Hydrophobic Particles. *Polym. Prepr. (Am. Chem. Soc., Div. Polym. Chem.)* **2001**, 42 (1), 246–247.
- Lin, Y.; Smith, T. W.; Alexandridis, P. Adsorption of Amphiphilic Copolymers on Hydrophobic Particles in Aqueous Media. *J. Disp. Sci. Technol.*, in press.
- Grieser, F.; Drummond, C. J. The Physical Properties of Self-Assembled Surfactant Aggregates As Determined by Some Molecule Spectroscopic Probe Techniques. *J. Phys. Chem.* **1998**, 92, 5580–5593.
- Alexandridis, P.; Holzwarth, J. F.; Hatton, T. A. Micellization of Poly(Ethylene Oxide)-Poly(Propylene Oxide)-Poly(Ethylene Oxide) Triblock Copolymers in Aqueous Solutions: Thermodynamics of Copolymer Association. *Macromolecules* **1994**, 27, 2414–2424.
- Lin, Y.; Alexandridis, P. Cosolvent Effects on the Micellization of an Amphiphilic Siloxane Graft Copolymer in Aqueous Solutions. *Langmuir* **2002**, 18, 4220–4231.
- Karukstis, K. K.; Savin, D. A.; Loftus, C. T.; Dangelo, N. D. Spectroscopic Studies of the Interaction of Methyl Orange with Cationic Alkyltrimethylammonium Bromide Surfactants. *J. Colloid Interface Sci.* **1998**, 203, 157–163.
- Nivaggioli, T.; Alexandridis, P.; Hatton, T. A.; Yekta, A.; Winnik, M. A. Fluorescence Probe Studies on Pluronic PEO-PPO-PEO Triblock Copolymer Solutions as a Function of Temperature. *Langmuir* **1995**, 11, 730–737.
- Lakowicz, J. R. *Principles of Fluorescence Spectroscopy*; Plenum Press: New York, 1983.
- Alexandridis, P.; Yang, L. Micellization of Polyoxyalkylene Block Copolymers in Formamide. *Macromolecules* **2000**, 33, 3382–3391.
- Stepanek, P. *Data Analysis in Dynamic Light Scattering: The Method and Some Applications*; Clarendon Press: 1993.
- Alexandridis, P.; Nivaggioli, T.; Hatton, T. A. Temperature Effects on Structural Properties of Pluronic P104 and F108 PEO-PPO-PEO Block Copolymer Solutions. *Langmuir* **1995**, 11, 1468–1476.
- Gentle, T. E.; Snow, S. A. Adsorption of Small Silicone Polyether Surfactants at Air/Water Interface. *Langmuir* **1995**, 11, 2905–2910.
- Soni, S. S.; Sastry, N. V.; Aswal, V. K.; Goyal, P. S. Micellar Structure of Silicone Surfactants in Water from Surface Activity, SANS and Viscosity Studies. *J. Phys. Chem. B* **2002**, 106, 2606–2617.
- Turro, N. J.; Baretz, B. H.; Kuo, P. L. Photoluminescence Probes for the Investigation of Interactions between Sodium Dodecyl Sulfate and Water-Soluble Polymers. *Macromolecules* **1984**, 17, 1321–1324.
- Edwards, D. A.; Luthy, R. G.; Liu, Z. Solubilization of Polycyclic Aromatic Hydrocarbons in Micellar Nonionic Surfactant Solutions. *Environ. Sci. Technol.* **1991**, 25, 127–133.
- Evans, D. F.; Wennerstrom, H. *The Colloidal Domain*, 2nd ed.; Wiley-VCH: New York, 1999.
- Schmitz, K. S. *An Introduction to Dynamic Light Scattering by Macromolecules*; Academic Press: New York, 1990.
- Alexandridis, P.; Yang, L. SANS Investigation of Polyether Block Copolymer Micelle Structure in Mixed Solvents of Water and Formamide, Ethanol, or Glycerol. *Macromolecules* **2000**, 33, 5574–5587.
- Fried, J. R. *Polymer Science and Technology*; Prentice-Hall: New York, 1995.
- Meguro, K.; Ueno, M.; Esumi, K. In *Nonionic Surfactants: Physical Chemistry*; Schick, M. J., Ed.; Marcel Dekker Inc.: New York, 1987.
- Alexandridis, P. Poly(ethylene oxide)-Poly(propylene oxide) Block Copolymer Surfactants. *Curr. Opin. Colloid Interface Sci.* **1997**, 2, 478–489.